Photonuclear attenuation and XCOM cross sections in EGSnrc

E. S. M. Ali[1,†], E. Mainegra-Hing[2], and D. W. O. Rogers[1]

[1] Carleton Laboratory for Radiotherapy Physics, Department of Physics, Carleton University, Ottawa, Canada
[2] Ionizing Radiation Standards, National Research Council, Ottawa, Canada.
E-mails: eali@physics.carleton.ca
ernesto.mainegra-hing@nrc-cnrc.gc.ca
drogers@physics.carleton.ca
† Current affiliation: Department of Medical Physics
The Ottawa Hospital Cancer Centre, Ottawa, Canada.
Available at: `http://physics.carleton.ca/clrp/photonuclear_xcom`

December 29, 2014 Report CLRP 14–01

Contents

Abstract

Purpose: To develop two new features in the `EGSnrc` Monte Carlo system. The first is the option to account for photonuclear attenuation, which can contribute a few per cent to the total cross section at the higher end of the energy range of interest to medical physics. The second is the option to use the exact NIST XCOM photon cross sections as input. **Methods**: For the first feature, the photonuclear total cross sections are generated from the IAEA evaluated data. In the current first-order implementation, after a photonuclear event, there is no energy deposition or secondary particle generation. The implementation is validated against deterministic calculations and experimental measurements of transmission signals. For the second feature, before this work the default cross section data were from Storm and Israel [Atom. Data Nucl. Data **7**, 565 – 681 (1970)], and if the user explicitly requested XCOM, `EGSnrc` still used its own internal incoherent scattering cross sections, which differ by up to 2% from XCOM data between 30 keV and 40 MeV. After this work, the default in `EGSnrc` is changed from Storm and Isreal to XCOM, except for incoherent scattering. Additionally, XCOM incoherent scattering cross sections are made as an available option. Minor interpolation artifacts in pair and triplet cross sections are addressed. The photonuclear, incoherent, pair and triplet data are available for elements with atomic numbers from 1 to 100 and for photon energies from 1 keV to 100 GeV. **Results**: Both features are implemented and validated in `EGSnrc`. **Conclusions**: The two features are part of the standard `EGSnrc` distribution as of 2012 (V4.2.3.2).

keywords: `EGSnrc`, XCOM, photonuclear.

1 Introduction

The EGSnrc system[1,2] is extensively used in photon calculations for diagnostic and therapy applications. In this work we report on two new features in the code: the option to account for photonuclear attenuation and the option to use the exact NIST XCOM photon cross sections as input.

2 Photonuclear attenuation

The photonuclear giant dipole resonance spans the energy range from a few MeV to tens of MeV and can contribute up to 6% to the total cross section. In this work, photonuclear total cross sections for natural elements with atomic numbers from 1 to 100 are generated for EGSnrc using the comprehensive IAEA compilation of evaluated photonuclear data[3] (mostly the ENDF/B-VII.1 library). The isotopes considered for each element and the source of their data are available in a web report[4]. The abundances of the constituent isotopes are taken from NIST (http://www.nist.gov/pml/data/comp.cfm). The energy grid for the input data to EGSnrc has 200 points linearly equi-spaced between the lowest threshold energy among the constituent isotopes of the element and the highest energy that has data available. The interpolation to create the data for this energy grid is linear in both energy and cross sections – the same as the IAEA interpolation. Cross sections for mixtures and compounds are generated using the standard independent-atom mixing rules. Fig. 1 shows examples for the contribution of the photonuclear component to the total cross sections. Photonuclear attenuation can be included for the full geometry or on a region-by-region basis. If included, the photon mean

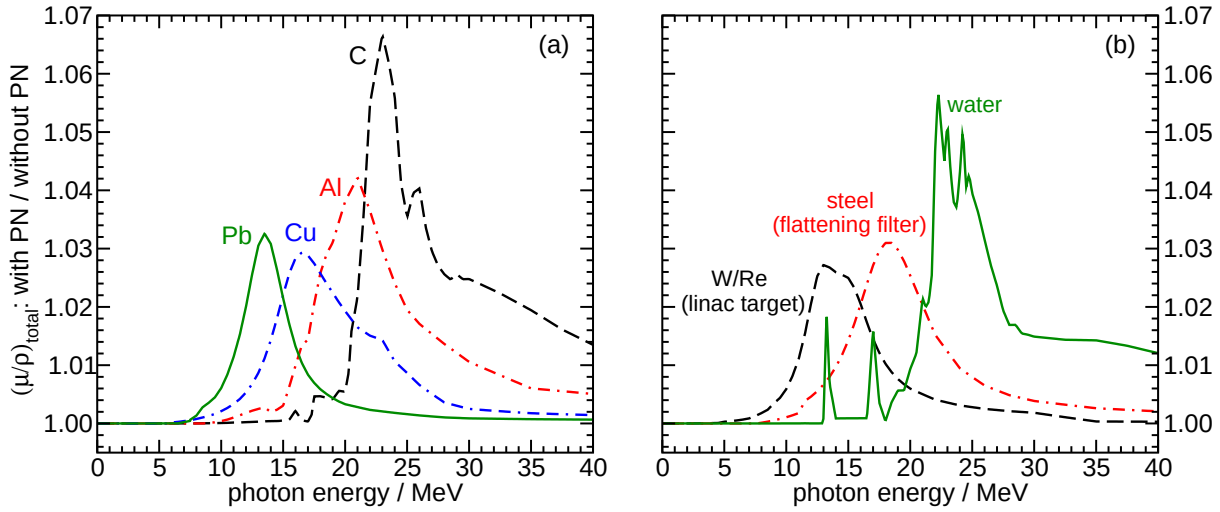

Figure 1: Ratio of the total mass attenuation coefficient, μ/ρ, with to without the photonuclear, PN, cross sections for elements of common interest (panel a), and for water and some components of an Elekta *Precise* linac head (panel b). Data are generated from within EGSnrc at runtime.

free path is shortened before the photon is transported to the interaction site. In the current first-order implementation, if the interaction is photonuclear, the photon is discarded without energy deposition or secondary particles generation. For the execution details, see Ref. [4].

To validate the implementation, EGSnrc is used to calculate transmission signals in narrow-beam geometry with and without photonuclear attenuation and the results are compared to deterministic calculations. Fig. 2 shows excellent agreement between the two calculation methods. There is ∼7% effect of photonuclear attenuation on the smallest transmission signals, which highlights the importance of including this option in EGSnrc. Fig 2

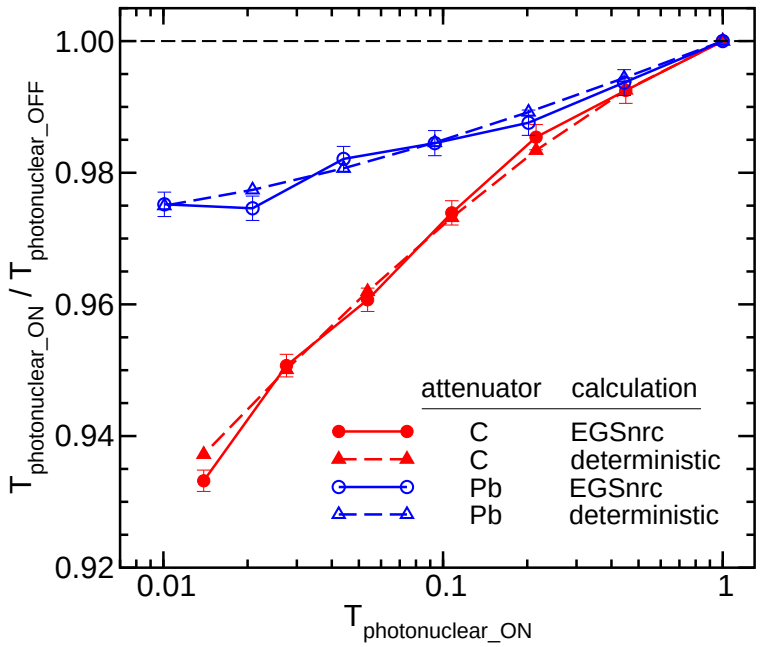

Figure 2: EGSnrc results versus deterministic calculations for the ratio of transmission, T, with to without the photonuclear component for graphite and lead attenuators. The photon source is a 30 MV beam.

In a previous study[5], transmission measurements were made on the research linac of the National Research Council Canada (NRCC) for different MV beams generated using different bremsstrahlung targets Fig. 3 shows the effect of including photonuclear attenuation on the agreement between the measured transmission signals and their respective EGSnrc calculations. Photonuclear attenuation is turned ON everywhere except in the detector. Accounting for photonuclear attenuation in the bremsstrahlung target leads to slight changes in the resulting photon spectrum, an example of which is shown in Fig. 4. Fig 3 Fig 4

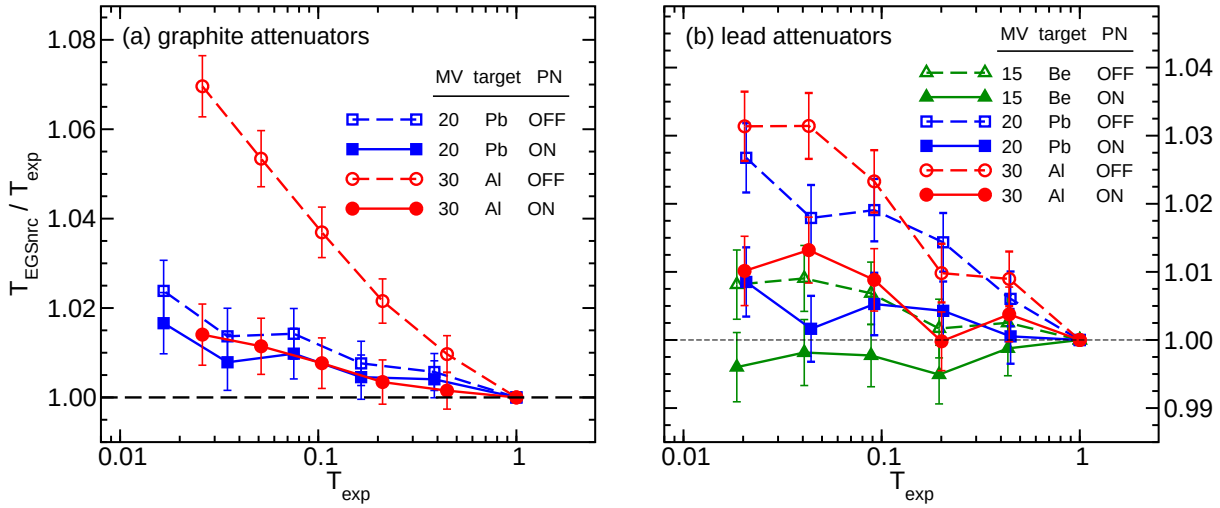

Figure 3: Improvements in the agreement between EGSnrc-calculated transmission data, T_{EGSnrc}, and measured data, T_{exp}, when photonuclear attenuation, PN, is accounted for in EGSnrc. Measured data are from Ali *et al*[5].

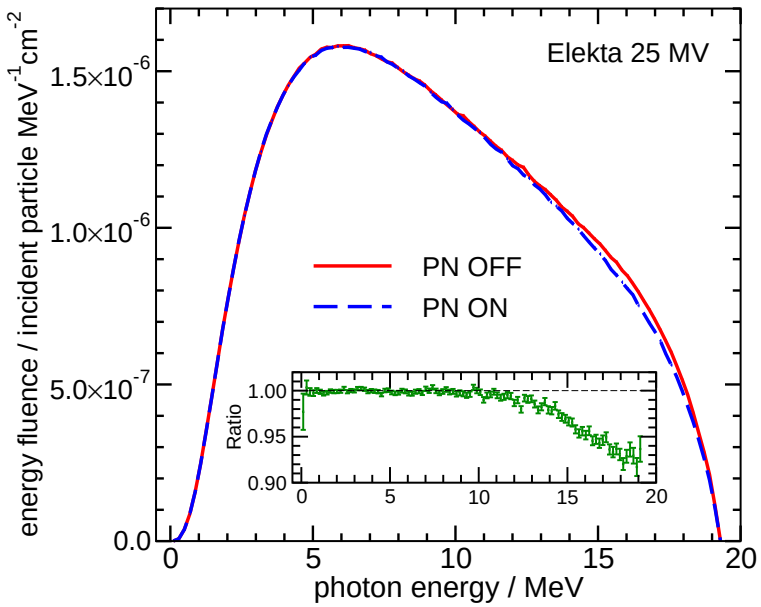

Figure 4: EGSnrc calculations for the effect on the energy fluence spectrum when photonuclear attenuation, PN, is modelled in the linac head components for an Elekta *Precise* 25 MV beam. The effect is smaller for lower MV beams.

3 XCOM cross sections

3.1 Incoherent scattering cross sections

Before this work, the default photon cross sections in EGSnrc were from Storm and Israel[6]. An option existed to use the NIST XCOM[7] data. However, if XCOM is requested, partial cross sections from XCOM are used for all interaction types except for incoherent scattering where

EGSnrc still uses its internal data. It is useful here to compare the basis of the incoherent scattering cross sections, $(\mu/\rho)_{incoh}$, for the internal model of EGSnrc versus XCOM.

EGSnrc calculates $(\mu/\rho)_{incoh}$ on the fly by (the equivalent of) integrating the differential cross sections used during transport. The relativistic impulse approximation (RIA)[8] is used. If requested, Doppler broadening, binding effects, radiative corrections and double Compton scattering are modelled. Doppler broadening uses the atomic and shell-wise Hartree-Fock Compton profiles by Biggs *et al*[9]. Radiative corrections and double Compton scattering are modelled using the corrections by Mork[10], which are based on the original derivation by Brown and Feynman[11]. Fig. 5 shows that radiative corrections plus double Compton scattering change the incoherent scattering cross section by -0.1% to +0.2%. On the other hand, XCOM $(\mu/\rho)_{incoh}$ values are calculated using the Klein-Nishina free-electron scattering, modified by the non-relativistic Hartree-Fock incoherent scattering functions[12,13,14]. Doppler broadening is not included and binding effects are included. Radiative and double Compton scattering corrections are the same as those in EGSnrc. Fig. 6a shows comparisons between $(\mu/\rho)_{incoh}$ calculated internally in EGSnrc versus XCOM data. The XCOM data are queried from the NIST website at the exact energies of the default 2000-point energy grid in EGSnrc to avoid interpolation artifacts. For graphite, the differences shown lead to 0.5% difference in mass energy absorption coefficient at 50 keV. Of the mature Monte Carlo codes, EGSnrc and PENELOPE[15] use the RIA to model incoherent scattering, while MCNP[16] and GEANT[17] use XCOM. The RIA is theoretically more accurate since it accounts for relativistic effects and Doppler broadening whereas XCOM does not.

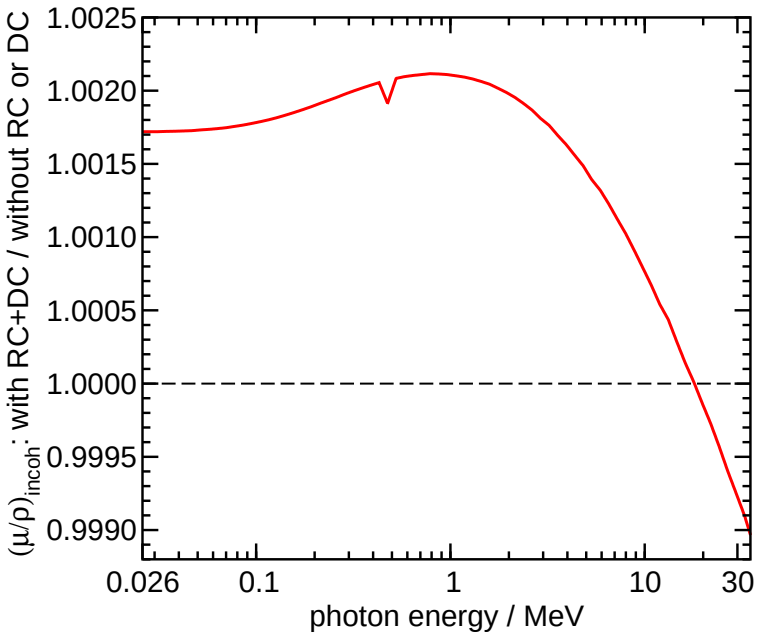

Figure 5: Ratio of EGSnrc incoherent scattering cross sections, $(\mu/\rho)_{incoh}$, with and without the radiative corrections, RC, and double Compton scattering, DC. The dip is an artifact at 511 keV. No data are available below 26 keV.

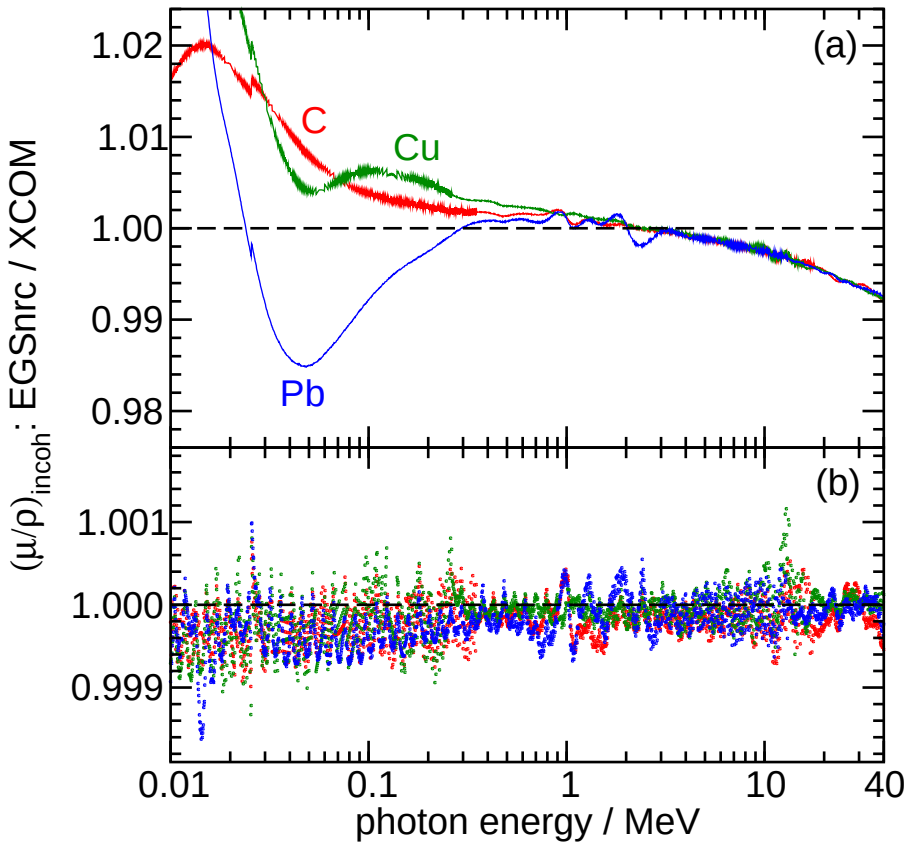

Figure 6: Ratios of the incoherent scattering cross sections, $(\mu/\rho)_{incoh}$, in EGSnrc to their respective XCOM values. In panel a, the EGSnrc data are calculated using its internal model, with binding effects, Doppler broadening, radiative corrections and double Compton scattering included. The differences increase to as much as 10% (not shown) at 10 keV for medium and high atomic number elements. Differences for elements lighter than graphite, such as beryllium, are up to 3% (not shown). The small discontinuity at ∼26 keV for all elements is because there is no radiative correction data below that energy. In panel b, the EGSnrc data are those added in this study.

In this work, $(\mu/\rho)_{incoh}$ is made as an available option in EGSnrc for applications that require full XCOM equivalency. Data are queried from the XCOM website at 150 energies logarithmically spaced between 1 keV and 100 GeV for elements with atomic numbers from 1 to 100. Since XCOM data already include radiative corrections and double Compton scattering, the data to be used as input in EGSnrc are divided by the relative magnitude of the internal EGSnrc radiative correction plus double Compton to allow for explicit modelling of these processes, which can result in additional particles. Fig. 6b shows the data from the current work. As a result, since EGSnrc V4.2.3.2 (2012), the default for photon cross sections is changed from Storm and Israel[6] to XCOM except for $(\mu/\rho)_{incoh}$ where the internal EGSnrc values are still used because it is theoretically more accurate and also for internal consistency because they are based on the integration of the differential cross sections that are actually used during the simulations. Additionally, XCOM incoherent scattering cross sections are

made as an available option. Therefore, for applications that require full XCOM equivalency (including $(\mu/\rho)_{incoh}$), the following three entries are required in the input file:

```
Compton cross sections= XCOM
Radiative Compton corrections= ON
Bound Compton scattering= SIMPLE
```

The third entry disables Doppler broadening and on-the-fly rejections due to binding effects, because XCOM data already include binding effects.

3.2 Pair and triplet cross sections

Before this work, XCOM pair and triplet data used at runtime in EGSnrc for energies other than those of the input grid differ from those queried directly from the XCOM website by up to 1.5%, as seen in Fig. 7a. This is due to the coarse fixed resolution of the input energy grid to EGSnrc. In this work, the input pair and triplet data to EGSnrc are re-created from the XCOM website using a variable-resolution energy grid to minimize interpolation artifacts. For pair data, 150 energies are used between 1.03 MeV and 100 GeV, and for triplet data, 115 energies are used between 2.05 MeV and 100 GeV. During runtime, the interpolation

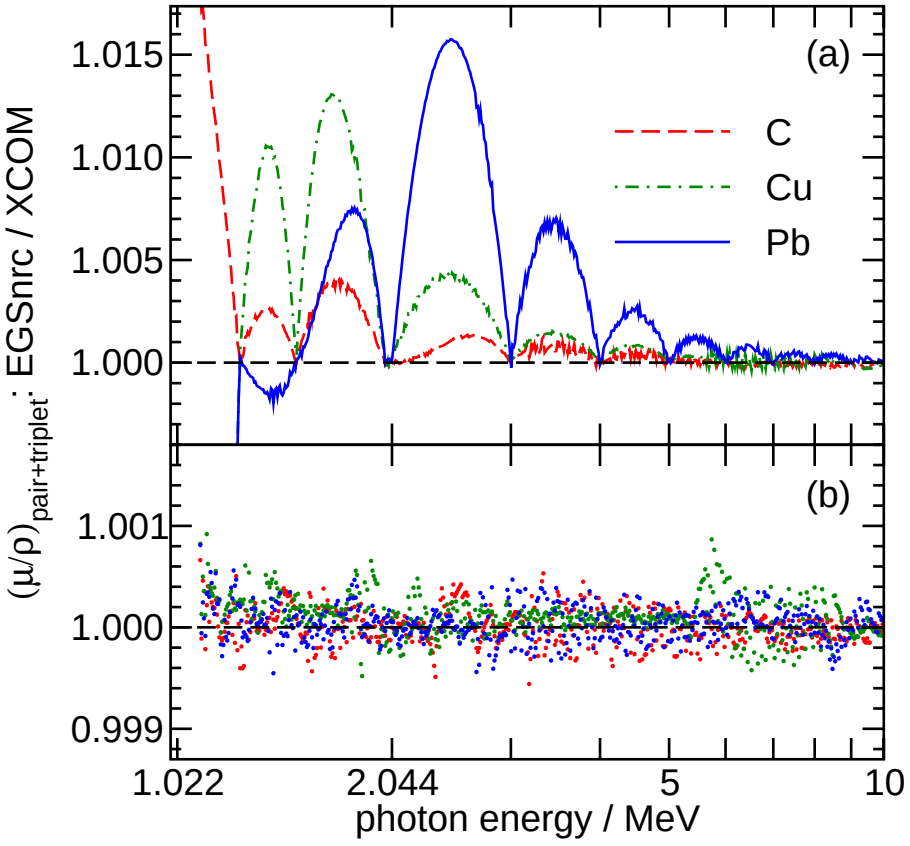

Figure 7: Ratios of the pair + triplet cross sections, $(\mu/\rho)_{pair+triplet}$, in EGSnrc to their respective XCOM values. Panel a: the old coarse input energy grid. Panel b: the new input energy grid.

remains the same: linear in $\ln[(1-E_{th}/E)^3\mu/\rho]$ versus $\ln(E)$, where E is the photon energy, μ/ρ is either pair or triplet cross section, and E_{th} is the corresponding production threshold (1.022 MeV for pair and 2.044 MeV for triplet production). As of EGSnrc V4.2.3.2 (2012), the refined pair and triplet data replace the old ones. Fig. 7b shows that the data from the current work.

3.3 Total cross sections

The combined effects of the changes in the incoherent, pair and triplet cross sections in EGSnrc are shown in Fig. 8. The data from the current work agree with XCOM data in general to within 0.1% (Fig. 8b). Although the overall effect of the details discussed above is comparable or only slightly larger than the uncertainty in the theoretical models upon which XCOM data are based, full XCOM equivalency is still needed for applications that are sensitive to small cross section differences – e.g., reproducing analytical half-value layer calculations[18], estimating photon cross section uncertainty[19], and comparison of simulation results from different Monte Carlo codes[18].

Fig 8

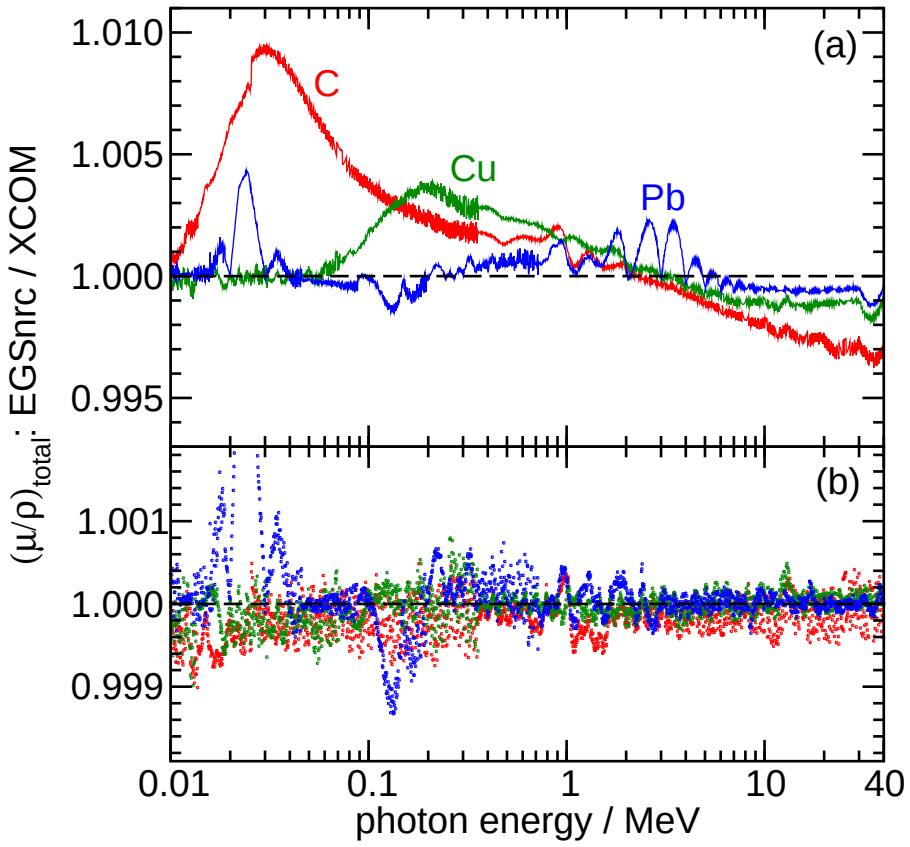

Figure 8: Ratios of the total photon cross sections, $(\mu/\rho)_{total}$, in EGSnrc (excluding the photonuclear cross sections of Sec.2) to their respective XCOM data before and after this work (panels a and b, respectively).

4 Summary

Two new features in EGSnrc are reported: the first is the option to account for photonuclear attenuation without modelling secondary particles nor their energy deposition, and the second is the option to use the exact XCOM photon cross sections as input. Both features are part of the standard EGSnrc distribution as of 2012 (V4.2.3.2).

5 Acknowledgments

We thank Frederic Tessier of NRCC for his guidance on automating the query of XCOM data from the NIST website. Elsayed Ali acknowledges funding from a Vanier CGS. Dave Rogers acknowledges funding from the CRC program, NSERC, CFI and OIT.

6 References

[1] I. Kawrakow, Accurate condensed history Monte Carlo simulation of electron transport. I. EGSnrc, the new EGS4 version, Med. Phys. **27**, 485 – 498 (2000). (p 3)

[2] I. Kawrakow, E. Mainegra-Hing, D. W. O. Rogers, F. Tessier, and B. R. B. Walters, The EGSnrc Code System: Monte Carlo simulation of electron and photon transport, NRC Technical Report PIRS-701 v4-2-3-2, National Research Council Canada, Ottawa, Canada. http://www.nrc-cnrc.gc.ca/eng/solutions/advisory/egsnrc/download_egsnrc.html, 2011. (p 3)

[3] IAEA, Handbook of photonuclear data for applications: cross sections and spectra, Technical Report TECDOC 1178, IAEA. Available at: http://www-nds.iaea.org/photonuclear, 2000. (p 3)

[4] E. S. M. Ali and D. W. O. Rogers, Implementation of photonuclear attenuation in EGSnrc, Technical Report CLRP 12–01 (14 pp), Carleton University, Ottawa, Canada. http://physics.carleton.ca/clrp/photonuclear, 2012. (pp 3 and 4)

[5] E. S. M. Ali, M. R. McEwen, and D. W. O. Rogers, Detailed high-accuracy megavoltage transmission measurements: A sensitive experimental benchmark of EGSnrc, Med. Phys. **39**, 5990 – 6003 (2012). (pp 4 and 5)

[6] E. Storm and H. I. Israel, Photon cross sections from 1 keV to 100 MeV for elements Z=1 to Z=100, Atomic Data and Nuclear Data Tables **7**, 565 – 681 (1970). (pp 5 and 7)

[7] M. J. Berger, J. H. Hubbell, S. M. Seltzer, J. Chang, J. S. Coursey, R. Sukumar, D. S. Zucker, and K. Olsen, XCOM: Photon cross section database (version 1.5), Technical report, NIST, Gaithersburg, MD, http://physics.nist.gov/xcom, 2010. (p 5)

[8] R. Ribberfors, Relationship of the relativistic Compton cross section to the momentum distribution of bound electron states, Phys. Rev. B **12**, 2067 – 2074 (1975). (p 6)

[9] F. Biggs, L. B. Mendelsohn, and J. B. Mann, Hartree-Fock Compton profiles for the elements, At. Data and Nucl. Data Tables **16**, 201 – 309 (1975). (p 6)

[10] K. J. Mork, Radiative Corrections: II. Compton Effect, Phys. Rev. **A 4**, 917 – 927 (1971). (p 6)

[11] L. M. Brown and R. P. Feynman, Radiative corrections to Compton scattering, Phys. Rev. **85**, 231 – 244 (1952). (p 6)

[12] J. H. Hubbell, W. J. Veigele, E. A. Briggs, R. T. Brown, D. T. Cromer, and R. J. Howerton, Atomic form factors, incoherent scattering functions, and photon scattering cross sections, J. Phys. Chem. Ref. Data **4**, 471 – 538 (1975). (p 6)

[13] J. H. Hubbell, Photon mass attenuation and energy-absorption coefficients from 1 keV to 20 MeV, Int. J. Appl. Radiat. Isot. **33**, 1269 – 1290 (1982). (p 6)

[14] J. H. Hubbell and S. M. Seltzer, Tables of x-ray mass attenuation coefficients and mass energy-absorption coefficients 1 keV to 20 MeV for elements Z = 1 to 92 and 48 additional substances of dosimetric interest, Technical Report NISTIR 5632, NIST, Gaithersburg, MD 20899, 1995. (p 6)

[15] J. Baro, J. Sempau, J. M. Fernandez-Varea, and F. Salvat, PENELOPE: an algorithm for Monte Carlo simulation of the penetration and energy loss of electrons and positrons in matter, Nucl. Inst. Meth. B **100**, 31 – 46 (1995). (p 6)

[16] F. B. Brown (Editor), MCNP—A general Monte Carlo N-particle transport code Version 5, Report LA-UR-03-1987, Los Alamos National Laboratory, Los Alamos, NM, 2003. (p 6)

[17] S. Agostinelli *et al.*, GEANT4 – a simulation toolkit, Nucl. Inst. Meth. A **506**, 250 – 303 (2003). (p 6)

[18] I. Sechopoulos, E. S. M. Ali, A. Badal, A. Badano, J. Boone, I. S. Kyprianou, E. Mainegra-Hing, M. F. McNitt-Gray, K. L. McMillan, D. W. O. Rogers, E. Samei, and A. C. Turner, Monte Carlo Reference Data Sets for Imaging Research: Abridged Report of the American Association of Physicists in Medicine Task Group No. 195, Med. Phys. , submitted (2014). (p 9)

[19] E. S. M. Ali, B. Spencer, M. R. McEwen, and D. W. O. Rogers, Towards a quantitative, measurement-based estimate of the uncertainty in photon mass attenuation coefficients at radiation therapy energies, Phys. Med. Biol. , submitted (2014). (p 9)